UNIVERSIDADE FEDERAL DO MARANHÃO

CENTRO DE CIÊNCIAS EXATAS E TECNOLOGIA

CURSO DE QUÍMICA BACHARELADO

BIONANOCOMPOSITOS BASEADOS EM ARGILAS LAMELARES CATIÔNICA E ANIÔNICA COMO DISPOSITIVOS DE LIBERAÇÃO CONTROLADA DE AMOXICILINA

Gabriel Pereira Souza

SÃO LUIS -MA

2019

UNIVERSIDADE FEDERAL DO MARANHÃO

CENTRO DE CIÊNCIAS EXATAS E TECNOLOGIA

CURSO DE QUÍMICA BACHARELADO

BIONANOCOMPOSITOS BASEADOS EM ARGILAS LAMELARES CATIÔNICA E ANIÔNICAS COMO DISPOSITIVOS DE LIBERAÇÃO CONTROLADA DE AMOXICILINA

Gabriel Pereira Souza

Monografia apresentada ao Curso de Química Bacharelado da Universidade Federal do Maranhão para obtenção do grau de Bacharel em Química.

Orientadora: Prof.ª Dr.ª Ana Clécia Santos de Alcântara

SÃO LUIS -MA

2019

Ficha gerada por meio do SIGAA/Biblioteca com dados fornecidos pelo(a) autor(a).
Núcleo Integrado de Bibliotecas/UFMA

Souza, Gabriel Pereira.
Bionanocompositos baseados em argilas lamelares catiônica e aniônica como dispositivos de liberação controlada de amoxicilina / Gabriel Pereira Souza. - 2019.
21 f.

Orientador(a): Ana Clécia Santos de Alcântara.
Curso de Química, Universidade Federal do Maranhão, Universidade Federal do Maranhão, 2019.

1. Amoxicilina. 2. Bionanocompositos. 3. Hidroxidos Duplos Lamelares. 4. Liberação controlada de fármacos. 5. Montmorillonita. I. Alcântara, Ana Clécia Santos de. II. Título.

Título: “BIONANOCOMPOSITOS BASEADOS EM ARGILAS LAMELARES CATIÔNICA E ANIÔNICA COMO DISPOSITIVOS DE LIBERAÇÃO CONTROLADA DE AMOXICILINA”

Gabriel Pereira Souza

Monografia julgada para obtenção do título

de **Bacharel em Química** em ___/___/___

Banca Examinadora

Prof.ª Drª. Ana Clécia Santos de Alcântara (Orientadora)

Universidade Federal do Maranhão – UFMA

Prof. Dr. Cícero Wellington Brito Bezerra

Universidade Federal do Maranhão – UFMA

Prof. Dr. Roberto Batista de Lima

Universidade Federal do Maranhão – UFMA

São Luís

2019

LISTA DE FIGURAS

LISTA DE TABELAS

SUMÁRIO

AGRADECIMENTOS

A minha orientadora, Drª Ana Alcântara, pela amizade, pela paciência e por todo o aprendizado durante esses anos, muito obrigado.

Aos meus amigos do Bionanos (e agregados), Rodrigo, Welton, Jeovan, Mayara, Vanessa, Thaylan, Wemerson, Elaine, Hiza, Elizaura e Bárbara, pela amizade, pelas brincadeiras e risadas, pelos cafés da tarde, por tudo que eu aprendi com vocês nesses anos, sem vocês muitos momentos não teriam sido tão alegres e divertidos, muito obrigado.

Aos meus amigos do Laboratório de Eletroquímica, pela amizade, pelo acolhimento todos esses anos e pelo excelente café sempre acompanhado de boas gargalhadas.

Aos meus colegas do LIM, por ter me recebido em seu laboratório, onde eu comecei minha iniciação cientifica.

Agradecer a Universidade Federal do Maranhão e todos os professores que ao longo desses anos contribuíram para a minha formação profissional e pessoal.

Agradecer principalmente aos meus pais, Welinton e Soraia, ao meu irmão, Felipe, pelo amor e pelo apoio durante todos esses anos, eu não seria nada sem vocês.

Obrigado!

RESUMO

No presente trabalho, bionanocompósitos à base de hidróxido duplo lamelares (HDL) e argila montmorillonita (Mt) como dispositivos de administração de medicamentos por via oral. Com esse objetivo, a amoxicilina, um antibiótico comumente indicado para diversos tipos de infecções, foi intercalada no espaço interlamelar da Mt e HDL, através de reações de troca catiônica e reconstrução, respectivamente, aproveitando a possibilidade de obter cargas positivas ou negativas na estrutura da amoxicilina, dependendo do pH da síntese. A partir das diversas técnicas de caracterização físico-químicas, i.e., DRX, FTIR, TG-DTA e SEM, foi possível inferir que moléculas de amoxicilina são dispostas em monocamada, cobrindo a superfície entre as lamelas de ambos os sólidos, neutralizando suas cargas, e consequentemente, conferindo uma melhora na estabilidade térmica do medicamento. Para melhorar o desempenho destes compostos de intercalação em meio ácido, por exemplo em fluído estomacal (pH 1,2), esses híbridos argila-amoxicilina foram incorporados em uma matriz de biopolímeros composto pelo polissacarídeo carboximetilcelulose e a proteína zeína, dando origem a esferas bionanocompósitos. Esses materiais bionanocompósitos as quais foram avaliados em função do tipo de composto de intercalação e da quantidade de zeína, mostraram boa compatibilidade entre seus componentes, oferecendo uma liberação mais controlada de amoxicilina em comparação com o respectivo híbrido ou mistura pura de biopolímeros, permitindo que a espécie ativa atinja o trato intestinal, melhorando a biodisponibilidade do fármaco.

Palavras-Chave: Montmorillonita, Hidroxidos Duplos Lamelares, Liberação controlada de fármacos, Bionanocompositos, Amoxicilina.

ABSTRACT

In the present work bionanocomposite materials based on layered double hydroxide and montmorillonite clay as drug delivery system for oral administration were prepared. With this aim, amoxicillin, an antibiotic commonly indicated for diverse kind of infections, was intercalated into Mt. or LDH interlayer space through cationic exchange and reconstruction reactions, respectively, taking advantage of the possibility to obtain positively or negatively charge in amoxicillin structure, depending on the pH of synthesis. From the diverse physicochemical characterization techniques, i.e. XRD, FTIR, TG-DTA and SEM was possible to infer that amoxicillin molecules are disposed as monolayer, covering the interlayer surface of both solids, neutralizing the charge of the lamellae, and consequently, conferring an improve in the thermal stability of the drug. In order to improve the performance of these intercalation compounds in acid media, e.g. stomach fluid (pH 1.2), these clay-amoxicillin hybrids were incorporated in a biopolymer matrix composed by carboxymethylcellulose polysaccharide and zein protein, giving rise bionanocomposite beads. These bionanocomposite materials, which were evaluated as a function of the type of intercalation compound and the amount of zein protein, showed good compatibility between their components, offering a more controlled release of amoxicillin compared to the respective hybrid or pure biopolymers blend, allowing that the active specie reaches the intestinal tract, improving the bioavailability of the drug.

Keywords: Montmorillonite, Layered double hydroxide, Drug delivery, Bionanocomposite, Amoxicillin.

Applied Clay Science 173 (2019) 35–45

Contents lists available at ScienceDirect

Applied Clay Science

journal homepage: www.elsevier.com/locate/clay

Research Paper

Bionanocomposites based on cationic and anionic layered clays as controlled release devices of amoxicillin

Ediana P. Rebitski[a,1], Gabriel P. Souza[b], Sirlane A.A. Santana[b], Sibele B.C. Pergher[a], Ana C.S. Alcântara[b,*]

[a] Universidade Federal do Rio Grande do Norte, Laboratório de Peneiras Moleculares-LABPEMOL, Instituto de Química, 59078-970 Natal, RN, Brazil
[b] Universidade Federal do Maranhão, Laboratório de Química de Interfaces e Materiais – LIM/Grupo de Pesquisa em Materiais Híbridos e Bionanocompósitos - Bionanos, DEQUI, 65080-805 São Luís, MA, Brazil

ARTICLE INFO

Keywords:
Montmorillonite
Layered double hydroxide
Drug delivery
Bionanocomposite
Amoxicillin

ABSTRACT

In the present work bionanocomposite materials based on layered double hydroxide and montmorillonite clay as drug delivery system for oral administration were prepared. With this aim, amoxicillin, an antibiotic commonly indicated for diverse kind of infections, was intercalated into Mt. or LDH interlayer space through cationic exchange and reconstruction reactions, respectively, taking advantage of the possibility to obtain positively or negatively charge in amoxicillin structure, depending on the pH of synthesis. From the diverse physicochemical characterization techniques, i.e. XRD, FTIR, TG-DTA and SEM was possible to infer that amoxicillin molecules are disposed as monolayer, covering the interlayer surface of both solids, neutralizing the charge of the lamellae, and consequently, conferring an improve in the thermal stability of the drug. In order to improve the performance of these intercalation compounds in acid media, e.g. stomach fluid (pH 1.2), these clay-amoxicillin hybrids were incorporated in a biopolymer matrix composed by carboxymethylcellulose polysaccharide and zein protein, giving rise bionanocomposite beads. These bionanocomposite materials, which were evaluated as a function of the type of intercalation compound and the amount of zein protein, showed good compatibility between their components, offering a more controlled release of amoxicillin compared to the respective hybrid or pure biopolymers blend, allowing that the active specie reaches the intestinal tract, improving the bioavailability of the drug.

1. Introduction

Nanostructured materials showing 2D lamellar structure based on inorganic solids such as layered double hydroxides (LDH) or montmorillonite nanoclay (Mt) are extensively studied mainly due to the high reactive surface, providing intercalation properties through anionic or cationic exchange reactions, respectively (Choy et al., 2007; Zhang et al., 2014; Calabrese et al., 2016; Calabrese et al., 2017; Bini and Monteforte, 2018; Sciascia et al., 2019). Within this large family of nanomaterials, it is worthy of note those prepared from the combination of layered clay minerals with biopolymers, that give rise to natural clay-polymer nanocomposites (Bergaya and Lagaly, 2006) or so-called bionanocomposite materials (Ruiz-Hitzky, 2003; Darder et al., 2007; Cavallaro et al., 2014; Bertolino et al., 2016; Allou et al., 2017; Cavallaro et al., 2018; Bertolino et al., 2018; Alcântara and Darder, 2018; Choi et al., 2018). These natural nanocomposites have received special attention because they meet important requirements for biocompatibility and biodegradability, which are of great interest for a wide variety of applications, such as in environmental remediation as adsorbent materials (Alcântara et al., 2014), in electrochemistry as potentiometric sensors (Darder et al., 2007), in food sector as biodegradable packaging (Alcântara et al., 2016), or in the biomedical sector as devices for drug controlled release (Aguzzi et al., 2007; Choy et al., 2007; Rives et al., 2014; Oliveira et al., 2017; Rebitski et al., 2018a, 2018b). Concerning this latter application, the versatility offered by bionanocomposite materials based on lamellar solids is mainly related to the ability of interlayer space to host active species (e.g. pharmaceuticals) and allow them to be gradually released.

Within this context, Mt. clay mineral is a phyllosilicate of the smectite clay family, characterized by a 2:1 charged layered silicate, where each layer consists of the repetition of octahedral alumina sheet which is sandwiched by two tetrahedral silica sheets, sharing oxygen

* Corresponding author.
E-mail address: ana.alcantara@ufma.br (A.C.S. Alcântara).
[1] Present address: Instituto de Ciencia de Materiales de Madrid, CSIC, Cantoblanco, 28049 Madrid, Spain.

https://doi.org/10.1016/j.clay.2019.02.024
Received 28 September 2018; Received in revised form 25 January 2019; Accepted 26 February 2019
Available online 13 March 2019
0169-1317/

atoms which are bonded to both sheets. Isomorphic substitution between the ions of Al^{+3} by Mg^{+2} or Fe^{+2} in the octahedral sheet, or Si^{+4} by Al^{+3} in the tetrahedral sheet generates a negative surface charge, which is compensated by cations in the interlayer region of the silicate (Olphen, 1977; Bergaya and Lagaly, 2006). These cations can be easily exchanged in aqueous media by other positively charged molecules such as polymers, biopolymers, pesticides, alkylammoniums or drugs, in order to be used for diverse applications (Gieseking, 1939; Bradley, 1945; Park et al., 2008; Darder et al., 2003; Calabrese et al., 2013; Alcântara et al., 2016;). On the other hand, LDH are known as anionic clays and consist of a large group of natural or synthetic materials that show their general formula $[M^{2+}_{(1-x)}M^{3+}_{x}(OH)_2](An^{-})_{x/n}\cdot zH_2O$, where M is a metal ion, and An^{-} is an interlayer anion that maintains the electroneutrality of the positively brucite-like sheets (Bergaya and Lagaly, 2006; Forano and Prevot, 2007). LDH are biocompatible, biodegradable and highly versatile platforms in which the combination with different kind of anionic molecules, including species of pharmaceutical interest, can be carried out by various synthesis procedures such as ion exchange reaction, co-precipitation and reconstruction, giving rise to multiple possibilities for obtaining different hybrid materials (He et al., 2006). Similarly to Mt clay mineral, LDH have been extensively exploited in order to obtain new materials for applications in catalysis, environmental remediation or as vector of drugs to improve their bioavailability and reduce side effects (Alcântara et al., 2010; Ribeiro et al., 2014a; Mei et al., 2017). However, both LDH and Mt. layered solids can show sensibility to changes of pH due to ions present in the media, mainly in acidic conditions in drug delivery applications (generally LDH due to basic nature), most of cases resulting in a burst release of the drug confined in its interlamellar structure in few minutes of contact (Alcântara et al., 2010; Parello et al., 2010; Rebitski et al., 2018a). This behavior is mainly related to exchange reactions with cations or anions present in the medium (e.g. H^{+}, Na^{+}, PO_4^{3-}), which making these materials, sometimes, a non-viable support for drugs via oral administration by itself (Zhang et al., 2006; Ribeiro et al., 2014a). In this sense, several studies demonstrated the efficiency of protection of hybrid materials based on the intercalation of drugs into Mt. or LDH by biopolymers, as a protective matrix to forming a controlled release bionanocomposite system. Thus, nanocomposites based on biopolymers and diverse clay-drug intercalation compounds were recently reported, for instance Mt-olanzapine (Oliveira et al., 2017), Mt-neomycin (Rebitski et al., 2018b) and LDH-ibuprofen (Ribeiro et al., 2014b).

Considering these premises, in this work Mt and LDH solids were used to encapsulate the amoxicillin drug. Amoxicillin (AMX) is a broad-spectrum β-lactam antibiotic and it is one of the most commonly used antibiotics via oral administration for the treatment of many infections, including dental postoperative, pneumonia, skin, throat and urinary infections, among others (Yu et al., 2017). AMX shows an amphoteric character, displaying different dissociation constants, which generate positively or negatively structural charges allowing its incorporation into either Mt or LDH solids, depending on the pH value (Fig. 1). Additionally, in order to form more efficient and stable release systems towards acidic conditions (e.g. pH of the first zone of gastrointestinal tract), the hybrids resulting from the intercalation of AMX into Mt. or LDH were combined with carboxymethylcellulose polysaccharide and zein protein. Carboxymethylcellulose (CMC) is a hydrophilic anionic polysaccharide obtained by the insertion of COOH groups into the molecular chains of cellulose. An interesting property of CMC is the ability to form beads by a crosslink process in aqueous media in the presence of Al^{+3} or Fe^{+3}. In contrast, zein (Z) is a protein obtained from maize, the presence of non-polar amino acids in its structure gives zein hydrophobic properties (Shukla and Cheryan, 2001; Paliwal and Palakurthi, 2014). These biopolymers are biocompatible, biodegradable and non-toxic, which allow their applications in a range of biomedical areas like tissue engineering, controlled drug release, among others (Marín et al., 2018). Recently, the combination of both biopolymers shown to be efficient as drug release systems for topical purposes, through its combination with sepiolite or montmorillonite-antibiotic hybrids (Rebitski et al., 2018b). Thus, the aim of this work is to study the synthesis and characterization of hybrid systems based on the intercalation of AMX into two lamellar inorganic solids of different structures (Mt and LDH), as well as the evaluation of the release AMX from bionanocomposite materials resulting of the combination of these clay-drug hybrids and carboxymethylcellulose-zein biopolymers.

2. Materials and methods

2.1. Starting materials and reagents

Zein and carboxymethylcellulose biopolymers, as well as amoxicillin antibiotic were purchased from Sigma-Aldrich. All the salts used were chemicals of analytical reagent grade: $Al(NO_3)_3\cdot 9H_2O$ (> 99%, Synth), $Zn(NO_3)_2\cdot 6H_2O$ (> 99%, Synth), NaOH (98%, Merck), NaCl (> 99%, Sigma-Aldrich), Na_2CO_3 (> 99%, Merck), $NaH_2PO_4\cdot H_2O$ (> 99%, (Sigma-Aldrich) and $CaCl_2$ (> 99%, Dinâmica). Homoionic sodium montmorillonite $(Na)_{0.33}(AlMg)_2(Si_4O_{10})(OH)_2\cdot nH_2O$) corresponds to a clay of Wyoming type supplied Southern Clay Products®, with a Cation Exchange Capacity (CEC) of 93 mEq per 100 g. Ethanol absolute grade was furnished from Synth.

2.2. Methods

2.2.1. Preparation of the montmorillonite-amoxicillin hybrid

For the preparation of montmorillonite-amoxicillin hybrid, 0.25 g of AMX in 10 mL of bidistilled water was homogenized by means of an ultrasonic bath for 30 min and the pH of the solution was reduced to 4.0 with a solution of HCl 0.1 M in order to obtain protonated amino groups in the drug structure. Simultaneously, 0.5 g of Mt was dispersed into 25 mL of water applying magnetic stirring to properly disperse the clay. The drug solution was added slowly in the suspension of Mt, forming a single bath. Then, the resulting mixture was kept in magnetic stirring for 24 h at room temperature. The solid product was isolated by centrifugation and washed 3 times with bidistilled water and dried overnight at 60 °C. The montmorillonite-amoxicillin hybrid material was denoted Mt-AMX.

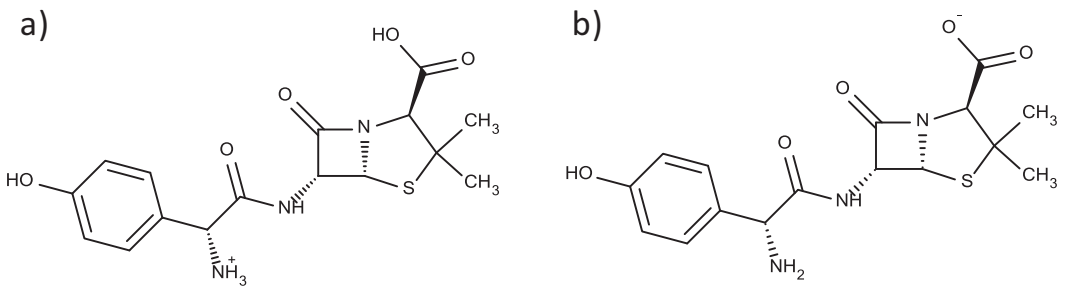

Fig. 1. Structure of amoxicillin (a) protonated up to pH 4, (b) deprotonated at pH ≈ 8.

2.2.2. Preparation of the $Zn^{2+}Al^{3+}/CO_3^{2-}$ layered double hydroxide

ZnAl LDH - carbonate [$[Zn_{0.67}Al_{0.33}(OH)_2](CO_3^{2-})_{0.33}{\cdot}nH_2O$] was prepared by co-precipitation method from a mixture of $Zn(NO_3)_2{\cdot}6H_2O$ (6.20 mmol) and 1.16 g of $Al(NO_3)_3{\cdot}9H_2O$ (3.10 mmol) which was dissolved in 400 mL of bidistilled water. The aqueous salt solution was added dropwise with a help of a burette to 100 mL of a solution 0.1 M of Na_2CO_3 previously prepared. Simultaneously, a solution of NaOH 1 M was also added dropwise to the aqueous system in order to keep a constant pH between 9 and 9.2 during the whole synthesis. The pH control was monitored by a pHmeter. The resulting suspension was vigorously magnetic stirred for 24 h and the solid product was isolated by centrifugation (4000 rpm), washed three times with bidistilled water, and dried overnight at 60 °C.

2.2.3. Preparation of the LDH ZnAl-amoxicillin hybrids

For the preparation of ZnAl LDH-amoxicillin hybrids, the reconstruction method was employed, where the ZnAl LDH previously prepared by co-precipitation, was calcined at 380 °C for 3 h under air flux to produce the corresponding layered double oxide (LDO). A solution containing 0.5 g of AMX in 50 mL of bidistiled water at pH 9, is added to 0. 25 g of calcined ZnAl LDH (theoretical ratio 1:0.5), is kept under magnetic stirring and nitrogen flow for 20 h. The solid is isolated by centrifugation, washed three times with bidistilled water, and dried overnight at 60 °C. The ZnAl LDH-amoxicillin hybrid material was labeled as LDH-AMX.

2.2.4. Preparation of carboxymethylcellulose-zein bionanocomposite beads

The carboxymethylcellulose-zein (CMC-Z) bionanocomposite beads were prepared following the previously reported method by (Alcântara et al., 2010) and (Rebitski et al., 2018b). In this case, different zein amounts (0, 0.4 and 1.0 g corresponding to 0, 25 and 50% with respect to total mass of biopolymers, respectively), together with 0 .1g of pure AMX or the necessary amount of Mt-AMX or LDH-AMX containing 0 .1g of AMX, were incorporated to 20 mL of ethanol – water (80%v/v). Once homogenized, this mixture is gradually added to CMC aqueous solution, where the concentration of CMC varied to reach a final total concentration of 2% of biopolymers (CMC:Z ratio 1:0, 1:0.25 and 1:1). After this step, the biopolymer system was added dropwise in a 5% solution of $AlCl_3$, in which they were kept under magnetic stirring for 20 min in order to favor the crosslinking process. Following that, the resulting beads were washed with approximately 200 mL of water to remove residual Al^{3+} ions and non-entrapped AMX. All materials were dried at room temperature. The CMC-Z*x* beads prepared by incorporation of pure AMX were denoted as CMC-Z*x*/AMX and those containing Mt-AMX and LDH-AMX intercalation compounds were labeled as CMC-Z/Mt-AMX and CMC-Z*x*/LDH-AMX, respectively, where "*x*" corresponds to the percentage of zein in the formulation.

2.3. Characterization

The prepared materials were characterized by X-ray diffraction (XRD) on a Bruker D2 Phaser using Cu radiation (λ = 1.54 Å), a 10 mA current, a 30 kV voltage and a LynxEye detector (192 channels). A 0.02° step size, 0.2 mm divergent slit, 0.4 s length and 1 mm anti-air-scattering screen were employed in the measurements. Infrared vibrational spectroscopic data were collected using a Perkin-Elmer Spectrum 65 FT-IR spectrometer coupled to a Perkin-Elmer Universal ATR sampling accessory. The analysis range was 400–4000 cm^{-1}. The thermal behavior of the prepared materials was evaluated by thermogravimetric (TG) and differential thermal analysis (DTA) in a DTG-60AH. The experiments were carried out under syntactic air atmosphere with a flux of 100 mL/min^{-1}, from room temperature to 900 °C at 10 °C/min^{-1} heat rate. The surface morphology was observed in a NOVA NANOSEM 230 utilizing low and high vacuum (10 to 100 Pa). The amount of drug in the intercalation compound was determined by CHN elemental chemical microanalysis in a LECO-CHNS-932 analyzer.

2.4. Estimation of AMX loading and encapsulation efficiency

To determine the AMX loading and the encapsulation efficiency in the beads, 0.2 g of beads were dispersed in 100 mL phosphate buffer at pH 6.8, and in order to ensure the disintegration of the bead and total release of the incorporated drug, the system was maintained under stirring for 24 h. Then, the solution was centrifuged, and the supernatant was analyzed in a UV-1800 spectrophotometer (Shimadzu) at an absorbance λ = 273 nm to determine the AMX content. The concentration of the drug was determined applying the Lambert-Beer law, and from these data the percentage of drug loading was calculated using the Eq. (1). This procedure was carried out by triplicate, and the maximum drug loading for each system was obtained. The encapsulation efficiency was calculated from Eq. (2) using the drug loading value (in mass) obtained for each system, and the theoretical loading, which is described as initial amount of drug added in the system (Babu et al., 2006)

$$\%\text{drug loading} = \frac{\text{amount of drug in beads (g)}}{\text{amount of beads (g)}} \times 100 \quad (1)$$

$$\%\text{encapsulation efficiency} = \frac{\text{drug loading (g)}}{\text{theoretical loading (g)}} \times 100 \quad (2)$$

2.5. Water uptake determination

The water uptake studies were performed by immersing 0.2 g of the biopolymer beads in 50 mL of bidistilled water or phosphate buffer at pH 6.8. At predetermined time interval the beads were withdrawn, after removing the excess of water, weighed in an analytical balance. The water uptake was calculated from the Eq. (3).

$$(g/g)\ \text{water uptake} = \frac{W_t - W_0}{W_0} \quad (3)$$

where W_0 and W_t are the initial and wet mass of beads at time t, respectively.

2.6. In vitro amoxicillin release studies

In vitro AMX release was conducted in conditions simulating the sequential pH changes that occur during the oral drug administration. For this, 0.2 g of beads was suspended in 100 mL of the chosen release medium and the temperature was kept at 37 °C under magnetic stirring (100 rpm). At appropriate intervals of time, an aliquot of 3 mL was withdrawn, and the amount of AMX released from the drug-loaded beads was evaluated by UV spectrophotometry (λ = 273 nm) in order to quantify the amount of drug released in the medium, applying the Lambert-Beer law. After that, the aliquot was added back to the solution, in order to maintain the constant volume. All the experiments were carried out in duplicate. The solutions employed to simulate the gastrointestinal fluids were used as follows: pH 1.2 (0 .1g NaCl and 0 .7ml HCl) for 2 h, acting as simulated gastric fluid; pH 6.8 (0. 03 g NaOH, 0. 40 g $NaH_2PO_4{\cdot}H_2O$ and 0. 62 g NaCl) for 2 h, simulating the first zone of intestinal fluid; and, pH 7.4 (prepared by adding 1 M NaOH to the pH 6.8 solution) for 4 h, simulating the second zone of intestinal fluid (Alcântara et al., 2010).

3. Results and discussion

3.1. Intercalation compounds characterization

It is well known that both Mt and LDH solids can be employed as host matrix for drug molecules through ionic exchange mechanisms, or in the case of LDH, its ability of regenerate the hydroxidic layers from their mixture of metal oxides obtained by calcination, through of adding an aqueous solution containing compensating anions,

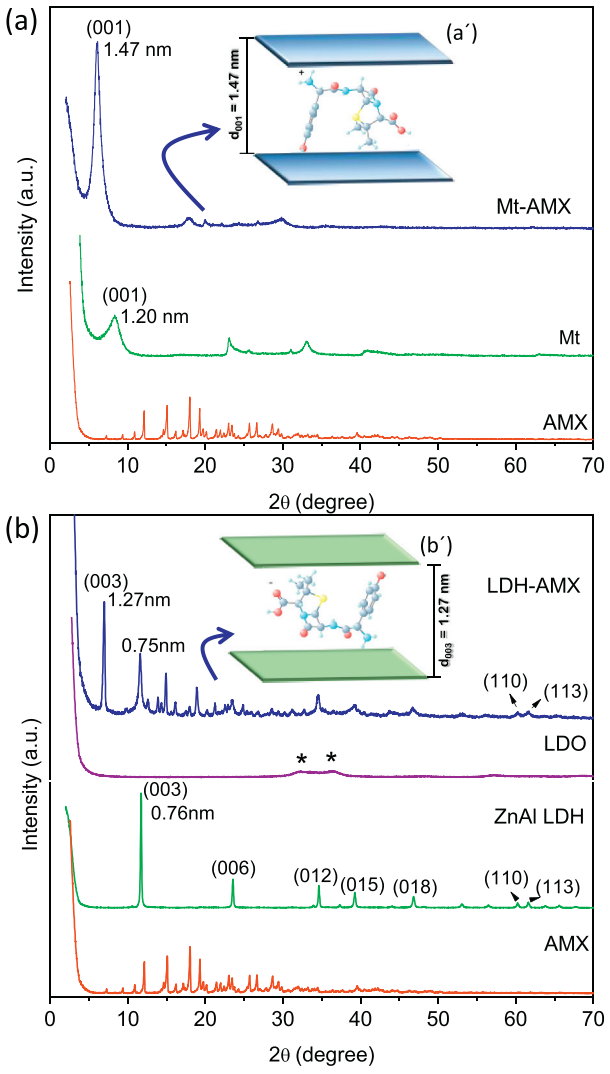

Fig. 2. XRD patterns of (a) pure amoxicillin, pristine Mt. and MMT-AMX hybrid prepared by ion-exchange reaction and (b) pure amoxicillin, pure ZnAl LDH–carbonate, ZnAl-LDO and LDH-AMX hybrid obtained by reconstruction method. The insert in (a′) and (b′) corresponds to the schematic representation of the possible accommodation of AMX into Mt. and LDH layers, respectively.

commonly known as “memory effect”. In the present case, the possible intercalation of AMX antibiotic in both solids was explored taking advantage of the dipolar structure of this drug which shows positive or negative charges, depending on the pH (Fig. 1). The XRD patterns of neat Mt, LDH and their derivatives after reaction with AMX are displayed in Fig. 2. From Fig. 2a, it can be clearly observed that the 001 reflection of neat Mt. shows an initial basal distance of 1.20 nm, which was shifted towards lower angles in 2θ, whereas a basal distance of 1.47 nm is showed in the hybrid material, indicating the presence of intercalated AMX into the interlayer space of Mt. clay. On the other hand, Fig. 2b, presents evidence of the formation of ZnAl LDH, where the carbonate ions are incorporated as anion charge compensation and the (003), (006), (012), (015), (018), (110) and (113) rational orders are evidenced (De De Roy et al., 2006), and its further transformation into the intended ZnAl LDO by calcination of the ZnAl LDH – carbonate material, demonstrating the presence of ZnO pointed as asterisk in the respective diffractogram. However, when this LDO is treated with a solution containing AMX in the anionic form (LDH-AMX), a clear shift in the position of the most intense peak, ascribed to the (003) reflection plane, towards lower angles in 2θ in comparison to that ZnAl LDH-carbonate is evidenced, confirming an AMX-intercalated phase. In this case, the resultant interlayer space changed from 0.76 nm in ZnAl LDH-carbonate to 1.27 nm in LDH-AMX hybrid, clearly suggesting the effective inclusion of drug molecules as anion charge compensations in the reconstruction of the layered hydroxide, where the well-separated (110) and (113) diffraction peaks at higher angles are also observed, confirming a well-crystallized lamellar structure in these materials. Although an important drug intercalated phase takes place in LDH-AMX, additional peaks related to the presence of crystalline AMX adsorbed on the external surface of the LDH were also observed, as well as the diffraction peak assigned to (003) reflection of ZnAl LDH-OH (d_{003} = 0.75), which could be attributed to hydroxyl intercalated ZnAl LDH phase. This latter evidence has been also observed by Wang et al. (2009) in studies about the possible reconstruction of calcined magnetic-LDH structure in presence of AMX.

Considering that the thickness of the Mt single layer and brucite-like layer of LDH are approximately 0.96 nm (Aranda and Ruiz-Hitzky, 1999) and 0.48 nm (Crepaldi and Valim, 1998), respectively, it is possible to deduce a basal spacing increase of around of 0.51 nm for the MMT-AMX and 0.79 nm for LDH-AMX materials, due to the AMX intercalation. Since a single AMX molecule shows dimensions of 0.74 × 0.43 × 0.94 nm (Wang et al., 2009), a probable accommodation of this antibiotic drug in the interlamellar region of the LDH and Mt can be proposed (Fig. 2a′ and b′, respectively), where the AMX molecules are arranged as monolayers in both cases, but in Mt-AMX hybrid it is suggested that the monolayer of AMX cations show a possible tilted angle as the drug molecule dimensions is larger than the gallery height. According to CHN chemical analyses, the amount of drug incorporated per gram of layered solid was 70 and 274 mEq of AMX for 100 g of Mt and LDH, respectively.

The infrared spectra of AMX, Mt., ZnAl LDH and their derivatives are shown in Fig. 3. In pristine Mt (Fig. 3a), the characteristic vibration modes of the 2:1 layered silicate are observed, where the OH stretching vibration band appears at 3625 cm^{-1}, δ_{HOH} of water molecules in the clay at 1628 cm^{-1}, the Si−O stretching bands are observed around the 1100–990 cm^{-1} range, and deformation bands assigned to (Al_2OH) and (MgAlOH) appear between 930 and 840 cm^{-1} region (Belver et al., 2012; Alcântara et al., 2016). In Mt-AMX spectrum, the vibration of both $\nu_{C\text{-}N}$ and $\delta_{N\text{-}H}$ of secondary amide groups from the drug seems to be overlapped with the typical vibrations modes of water molecules in Mt. at 1628 cm^{-1}, making very difficult the interpretation of possible interactions in this spectral zone. Nonetheless, it is observed that the band assigned to the $\nu_{N\text{-}H}$ at 3452 cm^{-1} in pure AMX is displaced towards lower wavenumber values showing in the hybrid material at 3406 cm^{-1}, which can be an indicative of possible electrostatic interactions between the negatively layer of Mt and the protonated amine groups from AMX. Otherwise, ZnAl LDH spectrum (Fig. 3b) exhibits a strong and broad band at 3382 cm^{-1} which is attributed to the stretching vibration of OH groups of LDH layers and interlayer water molecules. The observed band at 1357 cm^{-1} was ascribed to the asymmetrical stretching vibrations of CO_3^{-2} interlayer anions. In addition to those bands assigned to LDH, in the LDH-AMX spectrum, typical bands which can be attributed to the intercalated drug are observed. Comparing the pristine ZnAl LDH to and its hybrid compound, it is possible to evidence the presence of additional signals from AMX molecules. In this case, the intense band at 1770 cm^{-1} attributed to the ν(C = O) stretching vibration in free AMX disappears after incorporation into the LDH matrix, showing bands at 1523 and 1401 cm^{-1} in the hybrid materials that are assigned to the anti–symmetric (νas) and symmetric (νs) stretching vibration modes of −COO− groups, respectively (Bebu et al., 2011), corroborating the presence of the intercalated AMX in its anionic form.This effect is induced by the experimental condition (pH 9) that which promotes the stabilization of the drug molecule into LDH interlayer space in its anionic form, as similarly observed by other authors (Wang et al., 2017).

Fig. 4 shows the TG/DTA curves carried out under synthetic air atmosphere of the pristine layered solids and their hybrids Mt-AMX and

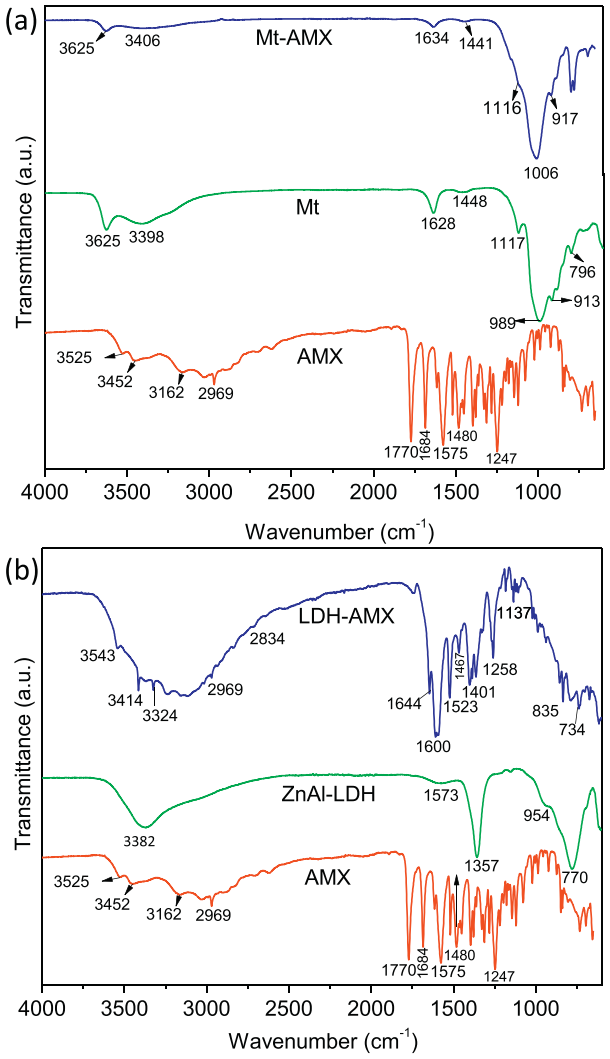

Fig. 3. Infrared spectra (4000–600 cm^{-1}) for (a) Mt-AMX and (b) LDH-AMX hybrids.

LDH-AMX. The thermal behavior of pure AMX (Fig. 4a) showed a mass loss of 17% corresponding to an endothermic peak at 98 °C, which is assigned to elimination of physically water molecules. Above 200 °C, the drug molecule starts its degradation process, being observed consecutive mass losses until approximately 650 °C, representing a mass loss of around 80%. These degradation processes were accompanied by two representative endothermic peaks at 398 and 587 °C. The starting Mt clay (Fig. 4b) show typical thermal curves of smectites, with a first mass loss correspondent to removal of physically adsorbed water at 68 °C, and the dissociation of water molecules bonded to the interlayer cations and structural hydroxyl groups, being evidenced in DTA curve an intense endothermic event at 634 °C (Aguzzi et al., 2014; Oliveira et al., 2017). The thermal stability of the Mt-AMX compound is very similar to the pristine Mt., where the AMX decompositions steps cannot be clearly defined, resulting in a more stable curve compared to the pure drug (Fig. 4c). Thus, Mt-AMX curves showed three representative mass losses, where the first one is related to elimination of physiosorbed water at temperatures below 100 °C, followed by a discrete exothermic event at 230 °C that can be associated with a possible decomposition of drug, and the dehydroxylation of the clay at temperatures between 600 and 800 °C. Although only few decomposition events of the AMX intercalated into Mt. clay are appreciated, it is important to highlight that similar results of TG/DTA curves involving intercalation of drugs into Mt. were recently reported (Oliveira et al., 2017; Rebitski et al., 2018a).

On the other hand, pure ZnAl LDH (Fig. 4d) shows good thermal stability up to 180 °C, where only physically adsorbed and interlamellar water elimination phenomena are observed, reflecting on the TG curve with a mass loss of approximately 18%. Events related to the partial dihydroxylation of brucite-like octahedral sheets together with the decomposition of carbonate anions located in the interlayer space of the LDH are evidenced between 180 and 320 °C, while those events assigned to total dihydroxylation of the material in order to form the ZnO and $ZnAlO_4$ spinel are showed up to 770 °C, accompanied with a mass loss of 15% (Constantino and Pinnavaia, 1995; De De Roy et al., 2006). In contrast to Mt-AMX curves (Fig. 4c), a significant change in the thermal behavior in the intercalated drug in LDH-AMX material is evidenced (Fig. 4e). In this case, LDH-AMX hybrid exhibit three main stages of thermal decomposition: i) up to 200 °C, showing an endothermic peak attributed to those physically adsorbed and interlamellar water; ii) in the 250–500 °C range, assigned to dihydroxylation of the LDH layers and partial oxidative decomposition of AMX, which is reflected as single exothermic peak centered at 378 °C; and iii) between 400 and 780 °C, which is likely attributed to the final decomposition of AMX and LDH. Despite the thermal stability of the drug is clearly improved after intercalation into LDH, where this latter acts as protector matrix for the AMX, it is relevant to mention that the steps of degradation of AMX molecule can be more evident in this case than compared to Mt-AMX (Fig. 4c), mainly due to the presence of possible drug crystals located on the external surface of the LDH, as indicated in XRD pattern (Fig. 2), as well as the higher amount of intercalated AMX in LDH than in Mt. silicate, as reported above.

The morphology of the LDH-AMX and Mt-AMX hybrids were examined by FE-SEM and the images are displayed in Fig. 5. SEM images of the Mt-AMX (Fig. 5a and b) show a typical morphology of hybrid materials based on montmorillonite (Darder et al., 2007; Alcântara et al., 2016; Carazo et al., 2018), where a layered aspect is evidenced. The LDH-AMX hybrid (Fig. 5c and d) shows a usual morphology so-called “rose sand” (Leroux and Taviot-Gueho, 2005), corroborating that the material was well reconstructed. In contrast, it is possible to appreciate the existence of particles located on the surface of the LDH, which could be attributed to the presence of AMX crystals on the external surface of the LDH, as pointed out by XRD results (Fig. 2).

3.2. Carboxymethylcellulose-zein/layered systems based on Mt-AMX or LDH-AMX hybrids

Bionanocomposite beads based on the incorporation of Mt-AMX or LDH-AMX intercalation compounds into a carboxymethycelullose-zein (CMC-Z) matrix with variable content of zein protein were prepared. For comparison, CMC-Z systems incorporating pure amoxicillin were also evaluated.

In order to evaluate the possible interaction between CMC and zein protein fraction, FTIR spectroscopy studies were carried out in CMC-Z blend (Fig. S1). It was observed that the spectrum of pure CMC-Z biopolymer blend prepared with 25% of zein (CMC-Z25), i.e. without drug content, (Fig. S1) shows bands at 3296 and 1037 cm^{-1}, which correspond to ν_{OH} (H_2O and −OH) and ν_{CO} (O−C−O) vibrations of ether groups from the polysaccharide. Typically, the band at 1638 cm^{-1} can be the result of a possible overlapping of the vibrations attributed to ν_{CO} amide I groups of zein and COO^- from the carboxylate groups in CMC, which can be related to possible interactions between the carboxylate groups and protonated amino groups from the cellulose derivative and the protein, respectively. These results are in accordance with those related in the literature for polysaccharide-protein interactions (Alcântara et al., 2010; Rebitski et al., 2018b).

The encapsulation efficiency and incorporated amounts of antibiotic drug incorporated in each system of release are listed in Table 1. For all systems studied, it is evidenced that increasing the zein content in the formulation also increases the amount of AMX loaded. This effect can be associated with the hydrophobic nature of this protein, favoring the

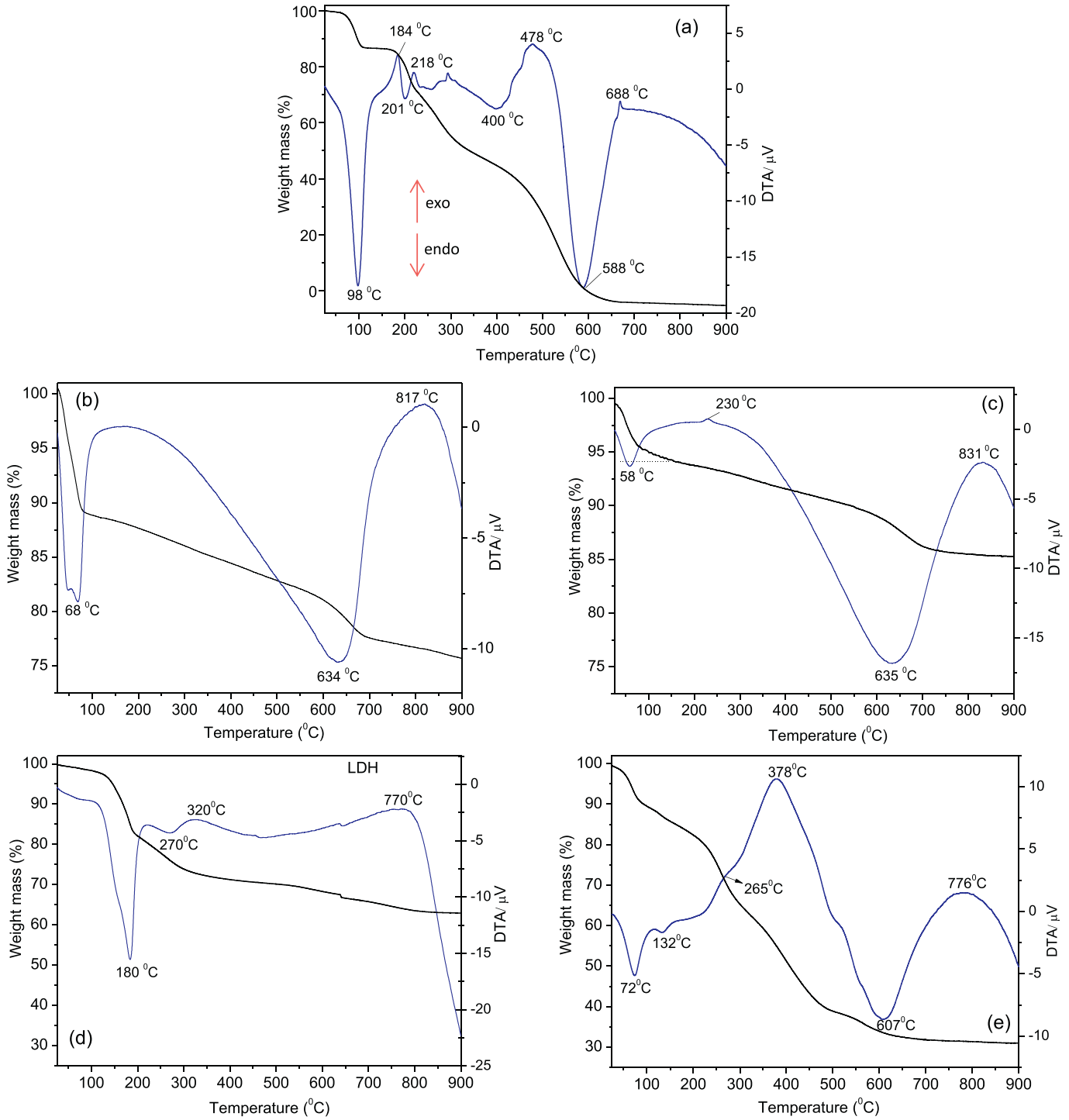

Fig. 4. TG (black lines) and DTA curves (blue lines) obtained for (a) amoxicillin, (b) Mt, (c) Mt-AMX, (d) ZnAl-LDH and (e) LDH-AMX. (For interpretation of the references to colour in this figure legend, the reader is referred to the web version of this article.)

entrapment of low water soluble drugs such as pure amoxicillin (Alcântara et al., 2010. Nevertheless, it is observed that the systems containing the drug previously immobilized in a lamellar matrix display higher encapsulation values in comparison to those systems which the AMX is directly associated to the biopolymer blend. A similar behavior was reported in the literature for alginate (Ribeiro et al., 2014b), alginate-zein (Alcântara et al., 2010) or chitosan–pectin (Ribeiro et al., 2014a) bionanocomposite systems that encapsulate ibuprofen or 5-ASA drugs intercalated in LDH, and such systems shown to be more stable and compatibles than those encapsulating the free drug.

The morphology of the synthetized beads was analyzed by FE-SEM and the micrographs are shown in Fig. 6. The images showed that all the systems have a rough and homogenous aspect. The system CMC-Z0/AMX, i.e., 0% w/w of zein (Fig. 6a and b) seems to show a higher porosity in comparison to other systems that incorporate zein. In this case, this system containing 50% (w/w) of protein (Fig. 6c and d) is characterized as a more compact material with a rough surface. Analogously to the CMC-Z systems that incorporate pure AMX, bionanocomposite beads containing Mt-AMX or LDH-AMX incorporated in a 50% (w/w) of protein matrix (Fig. 6e and f, respectively) show similar

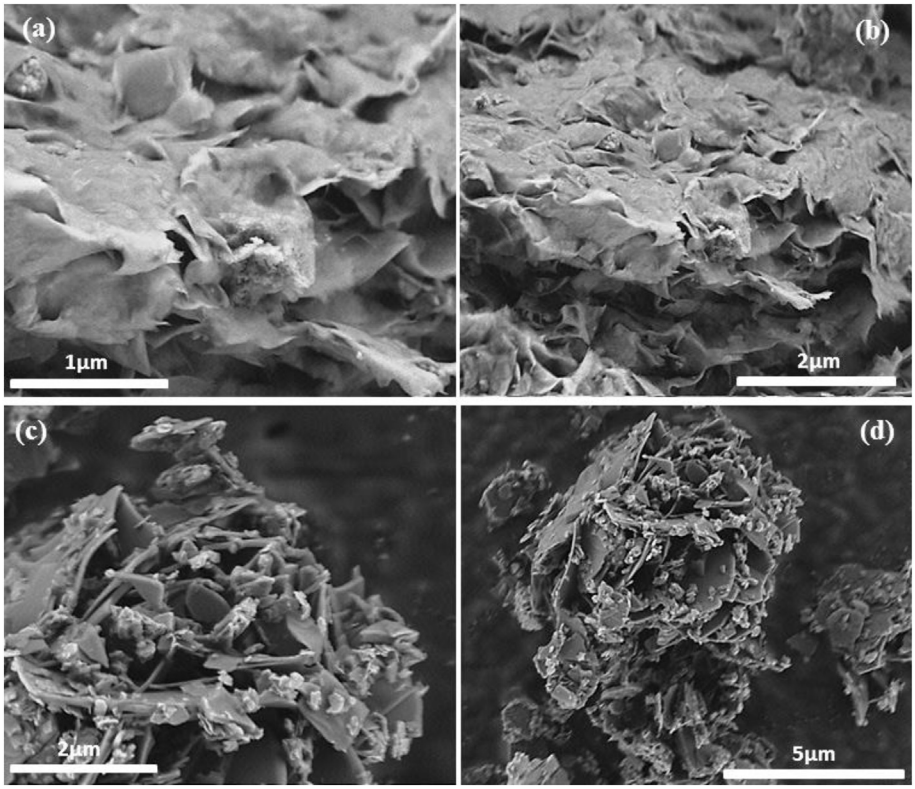

Fig. 5. SEM images of (a, b) Mt-AMX and (c, d) LDH-AMX hybrids.

surface morphologies in both cases, where a compact and free of cracks structure is observed in both cases, which suggests a good compatibility between the biopolymer and hybrid entities.

Taking into account that water uptake can play an important role in the release of drug from the bionanocomposite systems, this property was evaluated in the synthetized beads as a function of the exposure time in a pH 5.5 bidistilled water (Fig. 7a) and in a pH of 6.8 phosphate buffer media (Fig. 7b). It was observed that raising the exposure time in the aqueous media leads to increase the amount of water uptaken by all CMC-Z bionanocomposite systems. In the former case, CMC-Z beads that incorporate AMX (CMC-Z/AMX), showed some stability after 30 min of exposure, reaching a plateau at just over 5 g of absorbed water per g of bead for the CMC-Z0/AMX sample. For the bionanocomposite beads based on LDH-AMX, the presence of LDH particles in the CMC-Z beads seems to promote equilibrium of water absorption by the system after approximately 60 min of assay, as well as a significant decrease in water absorption values when compared to CMC-Z/AMX beads. In contrast, bionanocomposite beads that incorporate Mt-AMX hybrid showed higher values of water absorption compared to analogous materials based on LDH. Thus, the values can reach up to 4 g per g of material for the CMC-Z0/Mt-AMX after 180 min of experiment, and such effect is likely due to the hydrophilic character of the Mt clay, conferring to these materials a higher degree of swelling.

In contrast, when these beads are introduced in phosphate buffer (Fig. 7b), the values of water absorption are significantly increased after a few minutes of assay for all the tested systems, reaching almost 8.5 g of absorbed water per gram of bead in the CMC-Z0/AMX system. This behavior can be related to the pH of phosphate medium (6.8) that above the pKa of carboxylic groups from the CMC counterpart, which convert these groups into their ionized (COO—) and favors both the electrostatic repulsive force between negatively charged sites and the consequently release of Al^{3+} ions from the crosslinked CMC three-dimensional network, increasing the adsorption of water (Pourjavadi et al., 2006). However, the obtained amount of absorbed by the bionanocomposite beads which incorporate the AMX intercalated into LDH or Mt. layered solid are significantly lower compared to analogous materials prepared by direct incorporation of AMX in CMC-Z matrix. This fact indicates that the presence of the intercalation compounds confers to the bionanocomposite beads an improved chemical stability in the presence of salts, and this behavior could suggest that these biohybrid systems show different features as controlled drug release systems when compared with similar systems but based only on

Table 1
Encapsulation efficiency and amount of AMX loaded in different carboxymethycelullose-zein systems.

Formulation	Zein content in the system (%)	Loaded-AMX content (%)	Encapsulation efficiency (%)
CMC-Z0/AMX	0	13.3 ± 0.15	26.7 ± 0.45
CMC-Z0/Mt-AMX		12.8 ± 0.21	26.5 ± 0.69
CMC-Z0/LDH-AMX		15.7 ± 0.26	31.5 ± 0.31
CMC-Z25/AMX	25	18.7 ± 0.12	37.4 ± 0.22
CMC-Z25/Mt-AMX		19.9 ± 0.34	39.8 ± 0.87
CMC-Z25/LDH-AMX		20.8 ± 0.16	41.6 ± 0.44
CMC-Z50/AMX	50	20.4 ± 0.71	40.5 ± 0.38
CMC-Z50/Mt-AMX		22.3 ± 0.29	44.2 ± 0.20
CMC-Z50/LDH-AMX		26.0 ± 0.32	52.1 ± 0.53

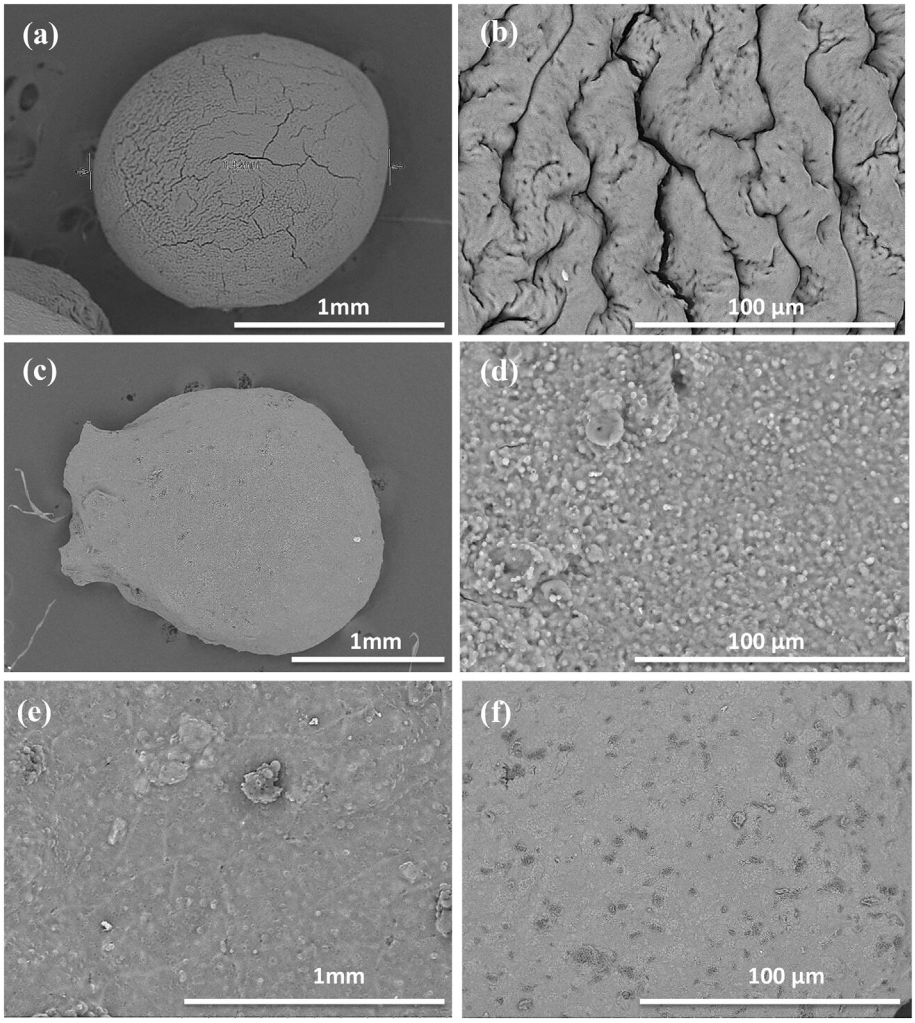

Fig. 6. SEM images of (a and b) CMC-Z0/AMX, (c and d) CMC-Z50/AMX, (e) CMC-Z50/Mt-AMX and (f) CMC-Z50/LDH-AMX bionanocomposite beads.

carboxymethylcellulose-zein. It is important to highlight that CMC-Z/LDH-AMX shows water uptake in phosphate buffer medium higher than comparable systems based on Mt-AMX. This behavior could be associated with the effect of phosphate anions acting as ion-exchange agents replacing the intercalated AMX^- molecules. Moreover, it is worth noting that the increase of zein in the blends causes a decrease in water absorption in all the beads tested, independent of the medium employed, and this effect can be associated to the hydrophobic character of this protein, which limits the passage of water molecules from the medium throughout the bead, as previously reported in similar systems based on alginate-zein (Alcântara et al., 2010).

3.3. In vitro release of amoxicillin from CMC-Z bionanocomposite beads

The release profiles of amoxicillin from LDH-AMX and Mt-AMX hybrids in CMC-Z bionanocomposite systems at different pH that simulate the gastrointestinal tract at 37 °C over 8 h of assay are shown in Fig. 8. The CMC-Z biopolymer blend showed to be a suitable material for the protection of the LDH-AMX hybrid. Thus, as observed in Fig. 8a, pure LDH releases > 90% of intercalated amoxicillin molecules in the first 30 min of assay, reaching 100% after 90 min, indicating that this kind of inorganic matrix is not suitable itself for oral purposes due the burst release caused by the fast dissolution of its layered structure in acidic media, i.e. stomach juice. Alternatively, when this hybrid is incorporated in CMC-Z blend, a clear protective effect of the LDH-AMX hybrid is observed, and only 15% of the drug is released in 30 min of assay for the bionanocomposite beads with 50% (w/w) of zein (CMC-Z50/LDH-AMX), which would allow the carrier to reach other parts of the body, such as intestinal juice at pH 6.8–7.4, releasing 80% of amoxicillin in the end of this process. Therefore, these results indicate that CMC-Z biopolymer blend are efficient in protecting the LDH-AMX material from the acid medium, promoting a controlled release of amoxicillin during its passage through the gastrointestinal tract. Analogous results were obtained for the bionanocomposite system based on Mt-AMX hybrid (Fig. 8b). On these terms, the montmorillonite clay showed a higher chemical stability in acidic media, probably due to the intrinsic structure and chemical composition, delivering around 85% of amoxicillin after 2 h of assay. The resulting release profile of the AMX is completely altered when the Mt-AMX is added to the biopolymer protective matrix. In this circumstance, it is observed that the bionanocomposite based on pure CMC, i.e. CMC-Z0/AMX, causes a delay in the release of the drug in simulated stomach juice in comparison to the hybrid alone, but in basic pH media (6.8 and 7.4), a fast release is evidenced reaching 100% of AMX released by the end of the simulation. Despite this, the presence of zein in the composition of the blend seems to favor a more sustained released, including basic pHs, a plateau at 55% of drug release up to 240 min of assay for CMC-Z25/Mt-AMX and at about 30% up to 150 min for CMC-Z50/Mt-AMX samples, increasing considerably the release of AMX after these times, i.e., when pH 7.4 is reached. This effect, which is evidenced for both LDH and Mt. bionanocomposite systems, can be associated with two main factors: i) the leaching of Al^{3+} cations from the biopolymer crosslinking network,

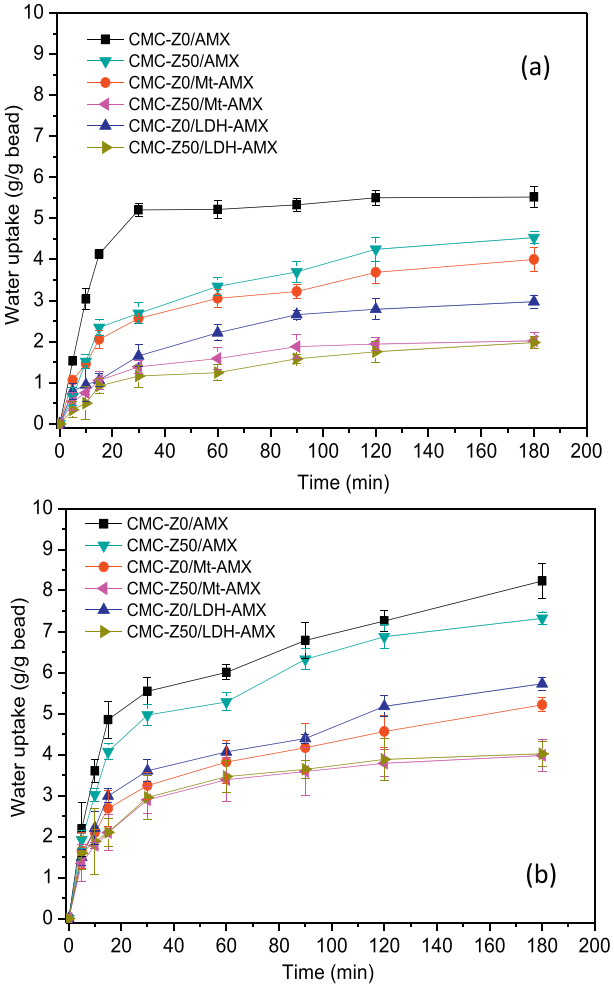

Fig. 7. Water uptake by CMC-Z bionanocomposite beads based on Mt-AMX and LDH-AMX prepared with 0 or 50% (w/w) of zein in contact with (a) pure bi-destilled water and (b) phosphate buffer at 6.8. Each value is the mean ± S.D. $n = 3$.

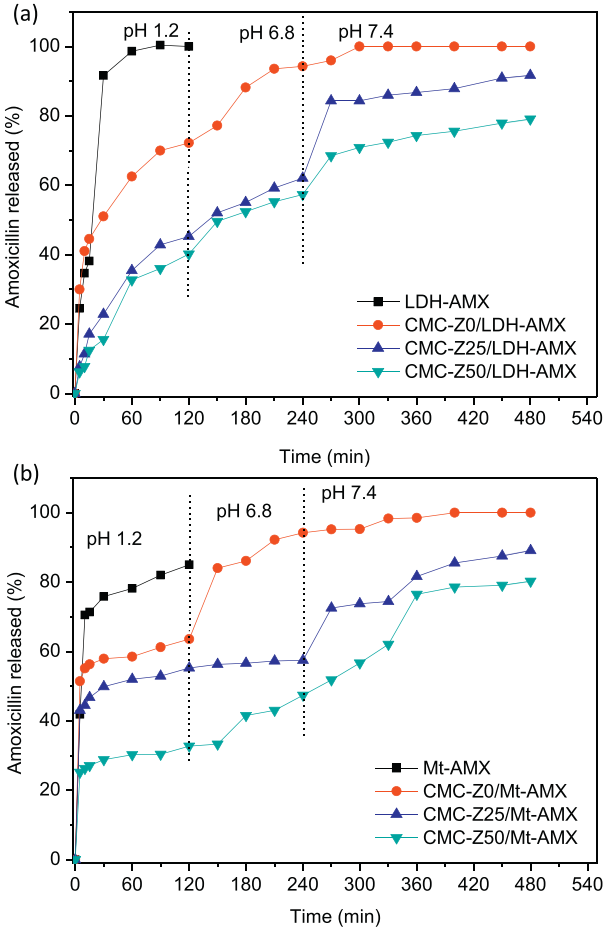

Fig. 8. Percentage of AMX released from (a) CMC-Z/Mt-AMX and (b) CMC-Z/LDH-AMX bionanocomposite beads, in conditions that simulate the gastrointestinal tract at 37 °C.

favoring the water adsorption in the system, and consequently, the release of the drug; and ii) the increase of the drug solubility in basic pH facilitating the release of the drug towards the medium (Pourjavadi et al., 2004). In addition, the possible contribution of ion exchange process between the intercalated negatively charged AMX and the phosphate anions present in the simulated intestinal medium should be not disregarded in the case of LDH-based materials, as previously discussed in the water uptake studies.

When comparing the controlled release systems of amoxicillin developed in this work with the release of a commercial amoxicillin capsule, as studied by Sahasathian et al. (2007) and Songsurang et al. (2011), it is observed that commercial amoxicillin is released rapidly, reaching its complete dissolution in approximately 1 h. In these same studies, biopolymer systems based on alginate, chitosan and ethyl cellulose were used to improve the control the release. Comparing these previous results involving commercial amoxicillin and biopolymer-amoxicillin (Sahasathian et al., 2007; Songsurang et al., 2011), with those obtained in this work, it is evident that the combination of amoxicillin-layered solids based intercalation compounds with biopolymers, seems to favor a more controlled release, likely due the contribution of inorganic solids (Mt and LDH) as efficient excipients for control in DDS systems, as already reported in the literature (Aguzzi et al., 2007; Viseras et al., 2010; Carretero and Pozo, 2010).

Due to the high complexity of the physical-chemical processes involving clay-based drug delivery systems, it becomes difficult to propose a releasing mechanism, since several factors can be related with the dissociation of the drug molecules from hybrid systems. In the case of bionanocomposite systems based on clays, ionic exchange reactions, diffusion and erosion processes, sensitive pH stimuli mechanisms, or even, a combination of them can take place in the drug release process (Siepmann et al., 2012; Jafarbeglou et al., 2016). In present case, the encapsulated drug seems to require additional time to be released from the LDH and Mt. inorganic matrices, since it is first expected that the beads undergo an swelling process, followed by an erosion or degradation of the biopolymer matrix caused by exposure to chemical substances present in the medium, and finally, the diffusion of the drug accommodated between the layers of the inorganic solid, resulting in a delay in the kinetics of diffusion of the drug, and consequently a more controlled release.

4. Conclusion

The intercalation of amoxicillin into interlayer space of montmorillonite clay and ZnAl-layered double hydroxide inorganic solids was successfully reached through cationic exchange mechanism and reconstruction reaction, respectively. From the XRD patterns, CHN analysis and FTIR spectroscopy results, it is possible to suggest that the amoxicillin molecules are disposed as a monolayer, covering the interlayer surface of both solids. In addition, the thermal analysis confirms a good thermal stability of the hybrid materials. Also in this study, it was possible to incorporate amoxicillin from the LDH-AMX and Mt-AMX intercalation compounds into a biopolymer matrix, forming bionanocomposite beads. These new bionanocomposite materials showed

good compatibility between their components, displaying a more controlled release of amoxicillin compared to the respective hybrid or biopolymers alone. The figures suggest that these new layered clay-based materials exhibit promising results for drug delivery systems, promoting a sustained release of amoxicillin, increasing the bioavailability of the drug by allowing the active specie to reach other areas of the body, such as the intestinal tract.

Acknowledgements

The authors acknowledge financial support from CNPq project 425730/2018-2, FAPEMA (UNIVERSAL 00961/18). E.P.R. and G.P.S. thank CAPES and FAPEMA for providing finantial support for master and undergraduate scholarships, respectively.

Appendix A. Supplementary data

Supplementary data to this article can be found online at https://doi.org/10.1016/j.clay.2019.02.024.

References

Aguzzi, C., Cerezo, P., Viseras, C., Caramella, C., 2007. Use of clays as drug delivery systems: possibilities and limitations. Appl. Clay Sci. 36, 22–36. https://doi.org/10.1016/j.clay.2006.06.015.

Aguzzi, C., Cerezo, P., Sandri, G., Ferrari, F., Rossi, S., Bonferoni, C., Caramella, C., Viseras, C., 2014. Intercalation of tetracycline into layered clay mineral material for drug delivery purposes. Mater. Technol. 29, B96–B99. https://doi.org/10.1179/1753555714y.0000000133.

Alcântara, A.C.S., Darder, M., 2018. Building up functional bionanocomposites from the assembly of clays and biopolymers. Chem. Rec. 18 (7–8), 696–712. https://doi.org/10.1002/tcr.201700076.

Alcântara, A.C.S., Aranda, P., Darder, M., Ruiz-Hitzky, E., 2010. Bionanocomposites based on alginate–zein/layered double hydroxide materials as drug delivery system. J. Mater. Chem. 20, 9495–9504. https://doi.org/10.1039/C0JM01211D.

Alcântara, A.C.S., Darder, M., Aranda, P., Ruiz-Hitzky, E., 2014. Polysaccharide–fibrous clay bionanocomposites. Appl. Clay Sci. 96, 2–8. https://doi.org/10.1016/j.clay.2014.02.018.

Alcântara, A.C.S., Aranda, P., Darder, M., Ruiz-Hitzky, E., 2016. Effective intercalation of zein into Na-montmorillonite: role of the protein components and use of the developed biointerfaces. Beilstein J. Nanotechnol. 7, 1772–1782. https://doi.org/10.3762/bjnano.7.170.

Allou, N.B., Saikia, P., Borah, A., Goswamee, R.L., 2017. Hybrid nanocomposites of layered double hydroxides: an update of their biological applications and future prospects. Colloid Polym. Sci. 295 (5), 725–747. https://doi.org/10.1007/s00396-017-4047-3.

Aranda, P., Ruiz-Hitzky, E., 1999. Poly(ethylene oxide)/$NH4^+$ -*smectite* nanocomposites. Appl. Clay Sci. 15 (1–2), 119–135.

Babu, V.R., Rao, K.S.V.K., Sairam, M., Naidu, B.V.K., Hosamani, K.M., Aminabhavi, T.M., 2006. pH sensitive interpenetrating network microgels of sodium alginate-acrylic acid for the controlled release of ibuprofen. J. Appl. Polym. Sci. 99, 2671–2678. https://doi.org/10.1002/app.22760.

Bebu, A., Szabó, L., Leopold, N., Berindean, C., David, L., 2011. IR, Raman, SERS and DFT study of amoxicillin. J. Mol. Struct. 993, 52–56. https://doi.org/10.1016/j.molstruc.2010.11.067.

Belver, C., Aranda, P., Martín-Luengo, M.A., Ruiz-Hitzky, E., 2012. New silica/alumina–clay heterostructures: properties as acid catalysts. Microporous Mesoporous Mater. 147, 157–166. https://doi.org/10.1016/j.micromeso.2011.05.037.

Bergaya, F., Lagaly, G., 2006. Chapter 1 general introduction: clays, clay minerals, and clay science. Dev. Clay Sci. 1, 1–18. https://doi.org/10.1016/s1572-4352(05)01001-9.

Bertolino, V., Cavallaro, G., Lazzara, G., Merli, M., Milioto, S., Parisi, F., Sciascia, L., 2016. Effect of the biopolymer charge and the nanoclay morphology on nanocomposite materials. Ind. Eng. Chem. Res. 55 (27), 7373–7380. https://doi.org/10.1021/acs.iecr.6b01816.

Bertolino, V., Cavallaro, G., Lazzara, G., Milioto, S., Parisi, F., 2018. Halloysite nanotubes sandwiched between chitosan layers: novel bionanocomposites with multilayer structures. New J. Chem. 2018 (42), 8384–8390. https://doi.org/10.1039/C8NJ01161C.

Bini, M., Monteforte, F., 2018. Layered double hydroxides (LDHs): versatile and powerful hosts for different applications. J. Anal. Pharm. Res. 7 (1), 00206. https://doi.org/10.15406/japlr.2018.07.00206.

Bradley, W.F., 1945. Molecular associations between montmorillonite and some polyfunctional organic liquids. J. Am. Chem. Soc. 67 (6), 975–981. https://doi.org/10.1021/ja01222a028.

Calabrese, I., Cavallaro, G., Scialabba, C., Licciardi, M., Merli, M., Sciascia, L., Liveri, M.L.T., 2013. Montmorillonite nanodevices for the colon metronidazole delivery. Int. J. Pharm. 457, 224–236. https://doi.org/10.1016/j.ijpharm.2013.09.017.

Calabrese, I., Cavallaro, G., Lazzara, G., Merli, M., Sciascia, L., Liveri, M.L.T., 2016. Adsorption 22 (2), 105–116. https://doi.org/10.1007/s10450-015-9697-1.

Calabrese, I., Gelardi, G., Merli, M., Liveri, M.L.T., Sciascia, L., 2017. Clay-biosurfactant materials as functional drug delivery systems: slowing down effect in the in vitro release of cinnamic acid. Appl. Clay Sci. 135, 567–574. https://doi.org/10.1016/j.clay.2016.10.039.

Carazo, E., Borrego-Sánchez, A., Sánchez-Espejo, R., García-Villén, F., Cerezo, P., Aguzzi, C., Viseras, C., 2018. Kinetic and thermodynamic assessment on isoniazid/montmorillonite adsorption. Appl. Clay Sci. 165 (1), 82–90. https://doi.org/10.1016/j.clay.2018.08.009.

Carretero, M.I., Pozo, M., 2010. Clay and Non-Clay Minerals in the Pharmaceutical and Cosmetic Industries Part II. Active Ingredients. Appl. Clay Sci. 47 (3–4), 171–181. https://doi.org/10.1016/j.clay.2009.10.016.

Cavallaro, G., Lazzara, G., Milioto, S., Parisi, F., 2014. Halloysite nanotubes as sustainable nanofiller for paper consolidation and protection. J. Therm. Anal. Calorim. 117 (3), 1293–1298. https://doi.org/10.1007/s10973-014-3865-5.

Cavallaro, G., Lazzara, G., Milioto, S., Parisi, F., Evtugyn, V., Rozhina, E., Fakhrullin, R., 2018. Nanohydrogel formation within the halloysite lumen for triggered and sustained release. ACS Appl. Mater. Interfaces 10 (9), 8265–8273. https://doi.org/10.1021/acsami.7b19361.

Choi, G., Eom, S., Vinu, A., Choy, J.H., 2018. 2D nanostructured metal hydroxides with gene delivery and theranostic functions; a comprehensive review. Chem. Rec. 1–22. https://doi.org/10.1002/tcr.201700091.

Choy, J.-H., Choi, J.-S., Oh, J.-M., Park, T., 2007. Clay minerals and layered double hydroxides for novel biological applications. Appl. Clay Sci. 36 (1), 122–132. https://doi.org/10.1016/j.clay.2006.07.007.

Constantino, V.R.L., Pinnavaia, T.J., 1995. Basic properties of $Mg^{2+}(1 - x)Al^{3+}$ x layered double hydroxides intercalated by carbonate, hydroxide, chloride and sulfateanions. Inorg. Chem. (4), 883–892. https://doi.org/10.1021/ic00108a020.

Crepaldi, E.L., Valim, J.B., 1998. Layered double hydroxides: structure, synthesis, properties and applications. Quím. Nova 21 (3), 300–311. https://doi.org/10.1590/s0100-40421998000300011.

Darder, M., Colilla, M., Ruiz-Hitzky, E., 2003. Biopolymer – clay nanocomposites based on chitosan intercalated in montmorillonite. Chem. Mater. 15 (20), 3774–3780. https://doi.org/10.1021/cm0343047.

Darder, M., Aranda, P., Ruiz-Hitzky, E., 2007. Bionanocomposites: a new concept of ecological, bioinspired, and functional hybrid materials. Adv. Mater. 19 (10), 1309–1319. https://doi.org/10.1002/adma.200602328.

De Roy, A., Forano, C., Besse, J.B., 2006. Layered double hydroxides: synthesis and post-synthesis modifications. In: Rives, V. (Ed.), Layered Double Hydroxides – Present and Future, Chapter 1, 1st edition. Nova Science Publishers, Inc., pp. 1–39.

Forano, C., Prevot, V., 2007. Enzyme-based bioinorganic materials. In: Ruiz-Hitzky, E., Ariga, K., Lvov, Y.M. (Eds.), Bio-Inorganic Hybrid Nanomaterials - Strategies, Syntheses, Characterization and Application, Chapter 15, 1 edition. Wiley-VCH, Weinheim, pp. 443–484.

Gieseking, J.E., 1939. The mechanism of cation exchange in the montmorillonite-beidellite-nontronite type of clay minerals. Soil Sci. 47, 1–14. https://doi.org/10.1097/00010694-193901000-00001.

He, J., Wei, M., Li, B., Kang, Y., Evans, D.G., Duan, X., 2006. Preparation of layered double hydroxides. In: Duan, X., Evans, D.G. (Eds.), Layered Double Hydroxides. Springer Berlin Heidelberg, Berlin, Heidelberg, pp. 89–119. https://doi.org/10.1007/430_006.

Jafarbeglou, M., Abdouss, M., Shoushtari, A.M., Jafarbeglou, M., 2016. Clay nanocomposites as engineered drug delivery systems. RSC Adv. 6, 50002–50016. https://doi.org/10.1039/C6RA03942A.

Leroux, F., Taviot-Gueho, C., 2005. Fine tuning between organic and inorganic host structure: new trends in layered double hydroxide hybrid assemblies. J. Mater. Chem. 15, 3628–3642.

Marín, T., Montoya, P., Arnache, O., Pinal, R., Calderón, J., 2018. Bioactive films of Zein/magnetite magnetically stimuli-responsive for controlled drug release. J. Magn. Magn. Mater. 458, 355–364. https://doi.org/10.1016/j.jmmm.2018.03.046.

Mei, X., Liang, R., Peng, L., Hu, T., Wei, M., 2017. Layered double hydroxide bio-composites toward excellent systematic anticancer therapy. J. Mater. Chem. B 5 (17), 3212–3216. https://doi.org/10.1039/c7tb00209b.

Oliveira, A.S., Alcântara, A.C.S., Pergher, S.B.C., 2017. Bionanocomposite systems based on montmorillonite and biopolymers for the controlled release of olanzapine. Mater. Sci. Eng. C 75, 1250–1258. https://doi.org/10.1016/j.msec.2017.03.044.

Olphen, H.V., 1977. 82. In: An Introduction to Clay Colloid Chemistry, 2nd ed. John Wiley & Sons, New York, London, Sydney, Toronto, pp. 236–237 Wiley-VCH Verlag GmbH & Co. KGaA. 10.1002/bbpc.197800022.

Paliwal, R., Palakurthi, S., 2014. Zein in controlled drug delivery and tissue engineering. J. Control. Release 189, 108–122. https://doi.org/10.1016/j.jconrel.2014.06.036.

Parello, M.L., Rojas, R., Giacomelli, C.E., 2010. Dissolution kinetics and mechanism of Mg-Al layered double hydroxides: a simple approach to describe drug release in acid media. J. Colloid Interface Sci. 351 (1), 134–139. https://doi.org/10.1016/j.jcis.2010.07.053.

Park, J.K., Choy, Y.B., Oh, J.M., Kim, J.Y., Hwang, S.J., Choy, J.H., 2008. Controlled Release of Donepezil Intercalated in Smectite Clays. Int. J. App. Pharm. 359 (1–2), 198–204. https://doi.org/10.1016/j.ijpharm.2008.04.012.

Pourjavadi, A., Sadeghi, M., Hosseinzadeh, H., 2004. Modified carrageenan Preparation, swelling behavior, salt- and pH-sensitivity of partially hydrolyzed crosslinked carrageenan-graft-polymethacrylamide superabsorbent hydrogel. Polym. Adv. Technol. 15 (11), 645–653. https://doi.org/10.1002/pat.524.

Pourjavadi, A., Barzegar, S., Mahdavinia, G.R., 2006. MBA-crosslinked Na-Alg/CMC as a smart full-polysaccharide superabsorbent hydrogels. Carbohydr. Polym. 66 (3), 386–395. https://doi.org/10.1016/j.carbpol.2006.03.013.

Rebitski, E.P., Aranda, P., Darder, M., Carraro, R., Ruiz-Hitzky, E., 2018a. Intercalation of

metformin into montmorillonite. Dalton Trans. 3185–3192. https://doi.org/10.1039/c7dt04197g.
Rebitski, E.P., Alcântara, A.C.S., Darder, M., Cansian, R.L., Gómez-Hortiguëla, L., Pergher, S.B.C., 2018b. Funcional carboxymethylcellulose/Zein bionanocomposite films based on neomycin supported on sepiolite or montmorillonite clays. ACS Omega 3, 13538–13550. https://doi.org/10.1021/acsomega.8b01026.
Ribeiro, L.N.M., Alcântara, A.C.S., Darder, M., Aranda, P., Araújo-Moreira, F.M., Ruiz-Hitzky, E., 2014a. Pectin-coated chitosan-LDH bionanocomposite beads as potential systems for colon-targeted drug delivery. Int. J. Pharm. 463 (1), 1–9. https://doi.org/10.1016/j.ijpharm.2013.12.035.
Ribeiro, L.N.M., Alcântara, A.C.S., Darder, M., Aranda, P., Araújo-Moreira, F.M., Ruiz-Hitzky, E., 2014b. Bionanocomposites containing magnetic graphite as potential systems for drug delivery. Int. J. Pharm. 477 (1), 55–563. https://doi.org/10.1016/j.ijpharm.2014.10.033.
Rives, V., del Arco, M., Martín, C., 2014. Intercalation of drugs in layered double hydroxides and their controlled release: a Review. Appl. Clay Sci. 88–89, 239–269. https://doi.org/10.1016/j.clay.2013.12.002.
Ruiz-Hitzky, E., 2003. Functionalizing inorganic solids: towards organic-inorganic nanostructured materials for intelligent and bioinspired systems. Chem. Rec. 3 (2), 88–100. https://doi.org/10.1002/tcr.10054.
Sahasathian, T., Kerdcholpetch, T., Chanweroch, A., Praphairaksit, N., Suwonjandee, N., Muangsin, N., 2007. Sustained release of amoxicillin from chitosan tablets. Arch. Pharm. Res. 30 (4), 526–531. https://doi.org/10.1007/BF02980229.
Sciascia, L., Casella, S., Cavallaro, G., Lazzara, G., Milioto, S., Princivalle, F., Parisi, F., 2019. Olive mill wastewaters decontamination based on organo-nano-clay composites. Ceram. Int. 45 (2), 2751–2759. https://doi.org/10.1016/j.ceramint.2018.08.155.
Shukla, R., Cheryan, M., 2001. Zein: the industrial protein from corn. Ind. Crop. Prod. 13 (3), 171–192. https://doi.org/10.1016/S0926-6690(00)00064-9.
Siepmann, J., Siegel, R.A., R., M.J. (Eds.), 2012. Fundamentals and Applications of Controlled Release Drug Delivery. Part III: Temporal Delivery Systems and Mechanisms, vol. 1 Springer Berlin.
Songsurang, K., Pakdeebumrung, J., Praphairaksit, N., Muangsin, N., 2011. Sustained release of amoxicillin from ethyl cellulose-coated amoxicillin/chitosan–cyclodextrin-based tablets. A A P S Pharm. Sci. Tech. 12 (1), 35–45. https://doi.org/10.1208/s12249-010-9555-0.
Viseras, C., Cerezo, P., Sanchez, R., Salcedo, I., Aguzzi, C., 2010. Current Challenges in Clay Minerals for Drug Delivery. App.Clay Sci. 48 (3), 291–295. https://doi.org/10.1016/j.clay.2010.01.007.
Wang, J., Liu, Q., Zhang, G., Li, Z., Yang, P., Jing, X., Jiang, Z., 2009. Synthesis, sustained release properties of magnetically functionalized organic–inorganic materials: Amoxicillin anions intercalated magnetic layered double hydroxides via calcined precursors at room temperature. Solid State Sci. 11 (9), 1597–1601. https://doi.org/10.1016/j.solidstatesciences.2009.06.
Wang, D., Peng, F., Li, J., Qiao, Y., Li, Q., Liu, X., 2017. Butyrate-inserted Ni–Ti layered double hydroxide film for H_2O_2-mediated tumor and bacteria killing. Mater. Today 20 (5), 238–257. https://doi.org/10.1016/j.mattod.2017.05.001.
Yu, K., Zhu, T., Wu, Y., Zhou, X., Yang, X., Wang, J., Fang, J., El-Hamshary, H., Al-Deyab, S.S., Mo, X., 2017. Incorporation of amoxicillin-loaded organic montmorillonite into poly(ester-urethane) urea nanofibers as a functional tissue engineering scaffold. Colloids Surf. B. 151 (1), 314–323. https://doi.org/10.1016/j.colsurfb.2016.12.034.
Zhang, H., Zou, K., Guo, S., Duan, D., 2006. Nanostructural drug-inorganic clay composites: structure, thermal property and in vitro release of captopril-intercalated Mg–Al-layered double hydroxides. J. Solid State Chem. 179, 1792–1801. https://doi.org/10.1016/j.jssc.2006.03.019.
Zhang, K., Xu, Z.P., Lu, J., Tang, Z.Y., Zhao, H.J., Good, D.A., Wei, M.Q., 2014. Potential for layered double hydroxides-based, innovative drug delivery systems. Int. J. Mol. Sci. 15 (5), 7409–7428. https://doi.org/10.3390/ijms15057409.